Paper 154

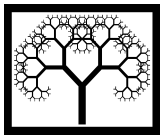

Proceedings of the Eleventh International Conference on Computational Structures Technology, B.H.V. Topping, (Editor), Civil-Comp Press, Stirlingshire, Scotland

Creep and Shrinkage Analysis of Curved Composite Beams Including the Effects of Partial Interaction

X. Liu[1], R.E. Erkmen[2] and M.A. Bradford[1]
[1] Centre for Infrastructure Engineering and Safety
Faculty of Engineering, The University of New South Wales, Sydney, Australia
[2] Centre for Built-Infrastructure Research, School of Civil and Environmental Engineering, University of Technology, Sydney, Australia

Abstract

This paper investigates the time-dependent creep and shrinkage behaviour of horizontally curved steel-concrete composite beams, including the effects of partial interaction existing between the concrete deck and steel girder. The flexibility of the shear connections in the radial direction, as well as in the tangential direction at the steel and concrete interface, are taken into account in the proposed formulation. The creep and shrinkage effects of the concrete deck including concrete age effects are considered by using the analytic age-adjusted effective modulus method. This method is efficient in converting the creep analysis into pseudo-elastic analysis. The accuracy and efficiency of the proposed approach is validated by comparing its results with available experimental results reported in the literature and those based on a more sophisticated but computationally less efficient ABAQUS shell finite element model. The effects of initial curvature and partial interaction on the time-dependent behaviour of curved composite beams under serviceability conditions are also elucidated and the slip effect due to warping is examined.

Keywords: composite beams, curvature, flexible, connections, creep, shrinkage, viscoelasticity.

1 Introduction

Composite steel and concrete beams which are curved in plan are used widely in highway bridges, particularly for motorway interchanges where high speeds require smooth changes in direction. Despite this, comparatively few analytical solutions have been reported on composite curved beams. An analytical formulation for horizontally curved composite bridge beams subjected to sustained loads and imposed deformation was developed by Giussani and Mola [1], in which it was assumed that there was full interaction between the steel girder and concrete deck. However, in composite beams, the flexibility of the shear connectors that join the

deck and the girder causes partial shear interaction which may significantly influence the deformations of composite beams [2,3]. Therefore, the well-known model of Newmark *et al.* [4] is commonly adopted for the analysis of straight composite beams with partial interaction in the longitudinal direction. For curved composite beams however, partial interaction not only exists in the tangential direction but also in the radial direction since radial deflection and twist of the beam occurs even under vertical loading. Erkmen and Bradford [5] developed a beam model that incorporates partial interaction in the tangential direction as well as in the radial direction in the elastic analysis of composite beams curved in plan and their model is adopted herein.

On the other hand, in structural engineering design, satisfying serviceability limit states is a vital component for the design of steel and concrete composite beams [6, 7]. In order to satisfy these serviceability requirements, an accurate assessment of the creep and shrinkage effects on the deflections is required. Much work has been reported on the time-dependent creep and shrinkage behaviour of straight composite beams with partial shear interaction. One of the earliest studies in this field was published by Tarantino and Dezi [8], in which a method was presented for the viscoelastic analysis of simply supported steel-concrete composite beams with flexible shear connectors. Later, they extended their method to study the long-term behaviour of composite continuous beams [9, 10] and shear-lag effects in composite beams [11]. In their analysis, the solution is achieved numerically by using a step-by-step procedure for the creep and shrinkage considerations. However, the numerical step-by-step procedure requires retaining of the full history of the strains and stresses which requires excessive computer storage [12]. Substantial simplification can be made to prevent the problem by using so-called algebraic methods such as the effective modulus method (EMM), age-adjusted effective modulus method (AEMM) and mean stress method (MSM), based on which creep and shrinkage effects can be determined in the current time step directly without integrating the full history. At the same time and independent of the Tarantino and Dezi study [8], Bradford and Gilbert [13] utilized a boundary value modelling approach for the analysis of simply supported steel-concrete composite beams based on the AEMM, and extended it to handling continuous beams [14]. Dezi *et al.* [15] performed a simplified creep analysis of continuous composite beams with flexible shear connectors. More recently, Ranzi and Bradford [16] presented a generic model for the time dependent analysis of steel-concrete composite beam with partial shear interaction by using the AEMM and MSM, while Amadio and Fragiacomo [17] evaluated creep and shrinkage effects in a composite beam with rigid as well as flexible connectors based on the AEMM. Erkmen and Bradford [18,19] considered viscoelastic Maxwell chain models for the time-dependent analysis of curved steel and concrete beams.

In this paper the object is to develop an accurate model for the creep and shrinkage analysis of steel-concrete composite beams with partial shear interaction while considering the effects of initial curvature. The work builds significantly on the kinematic model of Erkmen and Bradford [5] developed for curved composite

beams. However, in contrast to Erkmen and Bradford [18,19], the creep and shrinkage effects are included in this study by the AEMM which is computationally more efficient. In addition, we present a more detailed study on the warping induced slip. The proposed finite element formulation is validated by comparing the results with available experimental results reported in the literature and with those based on a sophisticated but computationally less efficient ABAQUS shell element model. The effects of initial curvature and partial interaction on the time-dependent behaviour of composite beams curved in plan are illustrated and the slip effect due to warping is clarified.

2 Kinematic relationships

2.1 Basic assumptions

Figure 1 shows a composite beam curved in plan for which the following assumptions are made.

- The steel girder is a doubly symmetric I-beam that is curved in plan.
- The deck has a rectangular cross-section and has the same initial curvature as the girder in the undeformed configuration.
- There is no uplifting between the girder and the deck.
- Radius of curvature is constant along the beam.
- The cross-section remains rigid and maintains its shape throughout the deformation, so that there is no distortion and no local buckling.
- The shear connection between the girder and the deck is flexible in both tangential and radial directions.
- Rotations, deflections and strains are small.
- The shear strain due to bending and warping are negligible, so that the shear strain on the cross-section is induced by uniform torsion only.

2.2 Axial systems and finite strain

A body attached curvilinear axis system is used to describe the geometry of the curved beam as shown in Figure 1. In the undeformed configuration, the axis system is in the position *oxys*. The axis *os* is oriented along the axial direction of the curved beam while the axes *ox* and *oy* are in the plane of the cross-section. The total deformations are considered to result from rigid translation due to displacements $u(s)$, $v(s)$, and $w(s)$ of the centroid along the tangential direction of the axes *ox*, *oy* and *os*, respectively, rotation of the cross section through an angle $\phi(s)$ about the axis *os*, superposed warping displacement of the whole cross-section due to non-uniform torsion, and displacement functions $\Omega_x(s)$, $\Omega_s(s)$ and $\Omega_\kappa(s)$ due to slip action in the radial and tangential directions in the horizontal plane and slip action induced by warping of the cross-section, respectively.

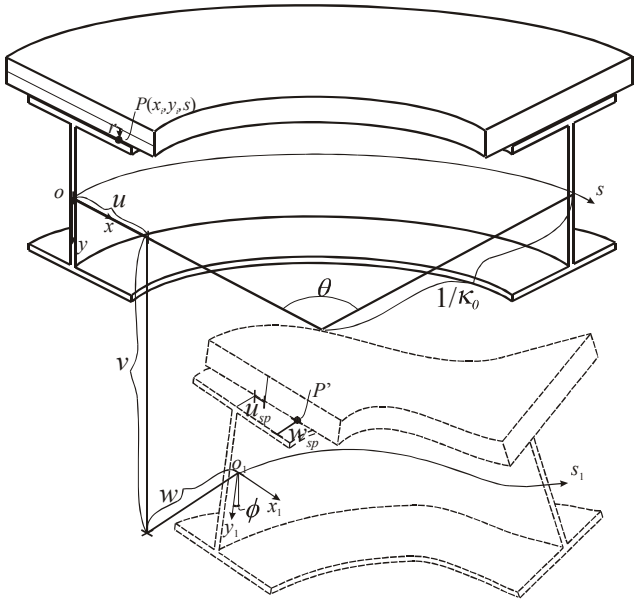

Figure 1: Coordinate system and deformations of the curved composite beam.

By adopting the Green-Lagrange strains and omitting the second and higher order small term, the non-zero normal strains at an arbitrary point *P* on the cross section of horizontal curved composite beam can be obtained [5] as

$$\varepsilon = \bar{w}' + \Omega_s' - \Omega_x \kappa_0 - x\left(\bar{u}'' + \bar{w}'\kappa_0 + \Omega_s'\kappa_0\right) - y\left(v'' - \kappa_0\phi\right) - \omega\left(\phi'' + v''\kappa_0 + \Omega_\kappa'\right), \quad (1)$$

in which $(\,)' \equiv \mathrm{d}(\,)/\mathrm{d}s$, $\bar{u}' = u' + w\kappa_0$ and $\bar{w}' = w' - u\kappa_0$. In Equation (1), κ_0 is the initial curvature of the beam about vertical axis and ω is the normalised section warping function. The functions Ω_x, Ω_s and Ω_κ are assumed positive for the girder and negative for the deck. The total slip displacements between the steel girder and concrete deck at the interface can be written as

$$u_{slip} = 2\Omega_x \quad (2)$$

for the radial direction and

$$w_{slip} = 2\Omega_s - 2\omega\Omega_\kappa \quad (3)$$

for the tangential direction. The non-zero shear strain due to the uniform torsion can be obtained [5] as

$$\gamma = -2r\left(\phi' + v'\kappa_0 + \Omega_\kappa\right), \quad (4)$$

where r is the perpendicular distance from the mid-surface of a plate segment to the point *P* on the cross-section.

3 Variational formulation of the equilibrium equations

The equilibrium equations can be obtained by using the principle of virtual work, which can be sated as

$$\delta\Pi=\int_L\int_{A_s}\delta\boldsymbol{\varepsilon}_s^{\mathrm{T}}\boldsymbol{\sigma}_s\mathrm{d}A\mathrm{d}s+\int_L\int_{A_c}\delta\boldsymbol{\varepsilon}_c^{\mathrm{T}}\boldsymbol{\sigma}_c\mathrm{d}A\mathrm{d}s+\int_L\int_b\delta\mathbf{d}_{slip}^{\mathrm{T}}\mathbf{q}_s\mathrm{d}x\mathrm{d}s-\sum\delta\mathbf{u}_Q^{\mathrm{T}}\mathbf{Q}-\int_L\delta\mathbf{u}_q^{\mathrm{T}}\mathbf{q}\mathrm{d}s=0\,, \quad (5)$$

in which the first two integrals are the internal virtual work due to the deformations of the steel girder and the concrete deck where A_s and A_c are the cross-sectional areas of the steel and concrete components respectively. Also in Equation (5), L is the total length of the beam, and $\boldsymbol{\varepsilon}_s,\boldsymbol{\sigma}_s,\boldsymbol{\varepsilon}_c$ and $\boldsymbol{\sigma}_c$ are the vectors of strain and stress components for the steel girder and concrete deck respectively. The third integral in Equation (5) is the internal virtual work due to the slip at the interface between the girder and the deck, in which $\mathbf{d}_{slip}$ and $\mathbf{q}_s$ are the vectors of the relative slip displacements and shear stresses between the deck and the girder respectively. The interface shear forces applied by the shear connectors are assumed to be continuously distributed, and b is the width of the effective interface surface. The last two terms in Equation (5) are the virtual work done by the external concentrated forces $\mathbf{Q}$ on the associated conjugate displacements $\delta\mathbf{u}_Q$ and the virtual work done by distributed member forces $\mathbf{q}$ on the associated conjugate displacements $\delta\mathbf{u}_q$.

3.1 Variation of strains

From Equations (1) and (4), the first variation of the normal and shear strains for both the steel girder and the concrete deck can be written as

$$\delta\boldsymbol{\varepsilon}_k=\mathbf{S}\mathbf{B}_k\delta\boldsymbol{\theta}\,, \quad (6)$$

in which index k can be changed to s for the steel girder and c for the concrete deck. The matrices $\mathbf{S}$ and $\mathbf{B}_k$ in Equation (6) are

$$\mathbf{S}=\begin{bmatrix}1 & x & y & \omega & 0\\ 0 & 0 & 0 & 0 & 2r\alpha\end{bmatrix} \quad (7)$$

and

$$\mathbf{B}_k=\begin{bmatrix}-\kappa_0 & 0 & 0 & 0 & 0 & 0 & 0 & 1 & 0 & 0 & 0 & a_k\kappa_0 & 0 & 0 & a_k & 0 & 0\\ {\kappa_0}^2 & 0 & -1 & 0 & 0 & 0 & 0 & -2\kappa_0 & 0 & 0 & 0 & 0 & 0 & 0 & a_k\kappa_0 & 0 & 0\\ 0 & 0 & 0 & 0 & 0 & -1 & 0 & 0 & \kappa_0 & 0 & 0 & 0 & 0 & 0 & 0 & 0 & 0\\ 0 & 0 & 0 & 0 & 0 & -\kappa_0 & 0 & 0 & 0 & 0 & -1 & 0 & 0 & 0 & 0 & 0 & a_k\\ 0 & 0 & 0 & 0 & -\kappa_0 & 0 & 0 & 0 & 0 & -1 & 0 & 0 & 0 & 0 & 0 & a_k & 0\end{bmatrix}, \quad (8)$$

where $a_s = 0.5$ for the steel girder, and $a_c = -0.5$ for the concrete deck.. In Equation (6), $\mathbf{\theta}$ is the displacement vector of the selected origin which can be written as

$$\mathbf{\theta} = \left\langle u \;\; u' \;\; u'' \;\; v \;\; v' \;\; v'' \;\; w \;\; w' \;\; \phi \;\; \phi' \;\; \phi'' \;\; 2\Omega_x \;\; 2\Omega_x' \;\; 2\Omega_s \;\; 2\Omega_s' \;\; 2\Omega_\kappa \;\; 2\Omega_\kappa' \right\rangle^{\mathrm{T}}. \quad (9)$$

3.2 Stresses

It is assumed that the material behaviour of the steel girder is linear elastic under service loads. Thus from elementary elasticity theory, the stresses of the steel girder can be written in term of strains as

$$\mathbf{\sigma}_s = \begin{Bmatrix} \sigma_s \\ \tau_s \end{Bmatrix} = \begin{bmatrix} E_s & 0 \\ 0 & G_s \end{bmatrix} \begin{Bmatrix} \varepsilon_s \\ \gamma_s \end{Bmatrix} = \mathbf{E}_s \mathbf{\varepsilon}_s, \quad (10)$$

where $\mathbf{E}_s$ is the matrix of material properties in which E_s and G_s are the Young's modulus and shear modulus of steel respectively. On the other hand, concrete deck is considered as an aging linear viscoelastic material. The viscoelastic response of the concrete is identical in both compression and tension as recommended in Gilbert [20], and Bazant and Oh [21] for stress level in compression less than about one half of the compressive strength of the concrete and in tension less than about one half of the tensile strength of the concrete. The stress states considered in this paper are assumed to remain in this stress range. By applying the superposition principle [22], the well-known integral constitutive relationship of time-dependent concrete behaviour can be written by using the creep function as

$$\begin{Bmatrix} \varepsilon_c(t) - \varepsilon_{sh}(t) \\ \gamma_c(t) \end{Bmatrix} = J(t,t_0) \begin{bmatrix} 1 & 0 \\ 0 & 2(1+\nu_c) \end{bmatrix} \begin{Bmatrix} \sigma_c(t_0) \\ \tau_c(t_0) \end{Bmatrix} + \int_{t_0^+}^{t} J(t,t') \begin{bmatrix} 1 & 0 \\ 0 & 2(1+\nu_c) \end{bmatrix} \begin{Bmatrix} \mathrm{d}\sigma_c(t') \\ \mathrm{d}\tau_c(t') \end{Bmatrix}, \quad (11)$$

where σ_c and τ_c are the time dependent concrete normal and shear stresses respectively, ε_{sh} is the stress independent shrinkage strain, t is the time at the casting of the concrete, t_0 is the time at initial loading in days, t_0^{+} indicates that the lower limit of the integration is taken after the initiation of loading, and $J(t, t')$ is the creep function defined as the strain at time t due to a constant unit stress acting from time t' to time t. The Poisson's ratio of concrete is taken as $\nu_c = 0.2$ and is assumed to be constant [23].

3.3 Variation of slip displacements and shear flow force at the interface

The first variation of slip displacements can be written as

$$\delta\mathbf{d}_{slip} = \left\langle \delta u_{slip} \quad \delta w_{slip} \right\rangle^{\mathrm{T}} = \mathbf{S}_{\Omega}\mathbf{B}_{\Omega}\delta\boldsymbol{\theta}\,, \tag{12}$$

in which

$$\mathbf{S}_{\Omega} = \begin{bmatrix} 1 & 0 & 0 \\ 0 & 1 & \omega \end{bmatrix}. \tag{13}$$

The elements of matrix $\mathbf{B}_{\Omega}$ can be written as

$$\mathbf{B}_{\Omega} = \begin{bmatrix} 0 & 0 & 0 & 0 & 0 & 0 & 0 & 0 & 0 & 0 & 0 & 1 & 0 & 0 & 0 & 0 & 0 \\ 0 & 0 & 0 & 0 & 0 & 0 & 0 & 0 & 0 & 0 & 0 & 0 & 0 & 1 & 0 & 0 & 0 \\ 0 & 0 & 0 & 0 & 0 & 0 & 0 & 0 & 0 & 0 & 0 & 0 & 0 & 0 & 0 & -1 & 0 \end{bmatrix}. \tag{14}$$

The behaviour of the stud shear connectors is assumed to be linear elastic; thus the shear flow force at the interface can be obtained in the terms of slip displacements as

$$\mathbf{q}_s = \left\langle q_{us} \quad q_{ws} \right\rangle^{\mathrm{T}} = \begin{bmatrix} \rho_u & 0 \\ 0 & \rho_w \end{bmatrix} \begin{Bmatrix} u_{slip} \\ w_{slip} \end{Bmatrix} = \boldsymbol{\rho}\mathbf{d}_{slip}\,, \tag{15}$$

where $\boldsymbol{\rho}$ is the matrix of the shear connection stiffnesses in both the radial and tangential directions. In Equation (15), ρ_u and ρ_w are the stiffnesses of the shear connections (with units of force/length^3) which can be defined as the shear stresses in the radial and tangential directions for a unit slip displacement, respectively.

3.4 External loadings

The external concentrated load vector $\mathbf{Q}$ can be written as

$$\mathbf{Q} = \left\{ Q_x \quad Q_y \quad Q_s \right\}^{\mathrm{T}}, \tag{16}$$

where Q_x and Q_y are the concentrated radial and vertical forces in the x and y directions, and Q_s is the external concentrated axial force in the s direction. Similarly, the external distributed loading vector acting on the member can be written as

$$\mathbf{q} = \left\{ q_x \quad q_y \quad q_s \right\}^{\mathrm{T}}, \tag{17}$$

where q_x , q_y and q_s are the counterpart actions to Q_x , Q_y and Q_s which are distributed in the s direction along the member. The external loads are assumed to act along the beams axis; accordingly the displacement $\mathbf{u}_Q$ and $\mathbf{u}_q$ at the points at

which loads **Q** and **q** act can be written in the terms of the displacements of the beam axis.

4 Creep and shrinkage analysis

4.1 Age-adjusted effective modulus method (AEMM)

Since time-dependent stress-strain relations based on the integral in Equation (11) requires a step-by-step numerical integration [12], simple and accurate algebraic methods such as the effective modulus method (EMM), mean stress method (MSM) and age-adjusted effective modulus method (AEMM) are often preferred [20], which replace the integral equations with simple algebraic equations. Instead of the step-by-step procedure, a single step analysis provides the stress-strain relations for the current time. Among these methods, the most general one is the AEMM developed by Bazant [24], while the other two simpler methods can be derived as the special cases of the AEMM. By using the AEMM, the concrete stresses at time *t* can be rewritten as [24, 25]

$$\boldsymbol{\sigma}_c = \begin{Bmatrix} \sigma_c(t) \\ \tau_c(t) \end{Bmatrix} = E_{ce}(t,t_0) \begin{bmatrix} 1 & 0 \\ 0 & 1/2(1+\nu_c) \end{bmatrix} \begin{Bmatrix} \varepsilon_c(t) - \varepsilon_{sh}(t) \\ \gamma_c(t) \end{Bmatrix} + \bar{\varphi} \begin{Bmatrix} \sigma_c(t_0) \\ \tau_c(t_0) \end{Bmatrix}, \tag{18}$$

in which, $\sigma_c(t_0)$ and $\tau_c(t_0)$ are the normal and shear stresses respectively which can be obtained from the instantaneous elastic analysis of composite beams curved in plan at time t_0. In Equation (18), $E_{ce}(t,t_0)$ is the age-adjusted effective modulus and $\bar{\varphi}$ is the creep effect factor, which can be written as

$$E_{ce}(t,t_0) = \frac{E_c(t_0)}{1+\chi(t,t_0)\phi_0(t,t_0)} \tag{19}$$

and

$$\bar{\varphi} = \frac{\phi_0(t,t_0)\left[\chi(t,t_0)-1\right]}{1+\chi(t,t_0)\phi_0(t,t_0)}, \tag{20}$$

where $E_c(t_0)$ is the elastic modulus of the concrete at time t_0, $\phi_0(t,t_0)$ is the creep coefficient defined as the ratio between the creep strain at time *t* and the initial strain at time t_0 and $\chi(t,t_0)$ is the aging coefficient which can be written as

$$\chi(t,t_0) = \frac{E_c(t_0)}{E_c(t_0) - R(t,t_0)} - \frac{1}{\phi_0(t,t_0)}, \tag{21}$$

in which $R(t,t_0)$ is the relaxation function. The AEMM is formulated for one step loading history; thus the load is applied at age t_0 and then is assumed to stay constant until the current time t. The stress expression for concrete is not only a function of the strain state at time t but also a function of the stress state that occurred at time t_0 and of the shrinkage deformations during time t. The response to multi-step loading histories can be obtained by superimposing the results for several one-step loading histories [26].

4.2 Finite element formulation

By using the virtual work principle in Equation (5), the equilibrium equations for a curved composite steel-concrete beam element at the current time t can be written as

$$\mathbf{Kd} = \mathbf{F}_{ext} + \mathbf{F}_c + \mathbf{F}_s, \tag{22}$$

where $\mathbf{K}$ is the displacement stiffness matrix, $\mathbf{d}$ is the nodal displacement vector, $\mathbf{F}_{ext}$ is the external load vector, $\mathbf{F}_c$ is the pseudo-load vector due to viscoelastic behaviour representing the history of the concrete since being loaded at time t_0 and $\mathbf{F}_s$ is the load vector due to the shrinkage effects. The stiffness matrix in Equation (22) can be written as

$$\mathbf{K} = \int_L \mathbf{N}^{\mathrm{T}} \left[\mathbf{B}_s^{\mathrm{T}} \left(\int_{A_s} \mathbf{S}^{\mathrm{T}} \mathbf{E}_s \mathbf{S} \mathrm{d}A \right) \mathbf{B}_s + \mathbf{B}_c^{\mathrm{T}} \left(\int_{A_c} \mathbf{S}^{\mathrm{T}} \mathbf{E}_c \mathbf{S} \mathrm{d}A \right) \mathbf{B}_c + \mathbf{B}_\Omega^{\mathrm{T}} \left(\int_b \mathbf{S}_\Omega^{\mathrm{T}} \boldsymbol{\rho} \mathbf{S}_\Omega \mathrm{d}x \right) \mathbf{B}_\Omega \right] \mathbf{N} \mathrm{d}s \tag{23}$$

in which the matrices of material properties for concrete $\mathbf{E}_c$ can be written explicitly as

$$\mathbf{E}_c = E_{ce}\left(t,t_0\right) \begin{bmatrix} 1 & 0 \\ 0 & 1/2\left(1+\nu_c\right) \end{bmatrix}. \tag{24}$$

The components at the right hand side of Equation (22) can be written as

$$\mathbf{F}_{ext} = \int_L \mathbf{N}^{\mathrm{T}} \mathbf{A}_q^{\mathrm{T}} \mathbf{q} \mathrm{d}s + \sum \mathbf{N}^{\mathrm{T}} \mathbf{A}_Q^{\mathrm{T}} \mathbf{Q}, \tag{25}$$

$$\mathbf{F}_c = -\int_L \mathbf{N}^{\mathrm{T}} \mathbf{B}_c^{\mathrm{T}} \left(\int_{A_c} \mathbf{S}^{\mathrm{T}} \bar{\varphi} \boldsymbol{\sigma}_0 \mathrm{d}A \right) \mathrm{d}s \tag{26}$$

and

$$\mathbf{F}_s = \int_L \mathbf{N}^{\mathrm{T}} \mathbf{B}^{\mathrm{T}} \left(\int_{A_c} \mathbf{S}^{\mathrm{T}} \mathbf{E}_c' \boldsymbol{\varepsilon}_{sh} \mathrm{d}A \right) \mathrm{d}s, \tag{27}$$

where the vectors of the instantaneous stress $\boldsymbol{\sigma}_0$ and the shrinkage strain $\boldsymbol{\varepsilon}_{sh}$ can be

written as

$$\boldsymbol{\sigma}_0 = \left\langle \sigma(t_0) \quad \tau(t_0) \right\rangle^{\mathrm{T}} \tag{28}$$

and

$$\boldsymbol{\varepsilon}_{sh} = \left\langle \varepsilon_{sh}(t) \quad 0 \right\rangle^{\mathrm{T}}. \tag{29}$$

In Equations (23) to (27), **N** is the finite element shape function matrix, which is obtained herein by interpolating the displacement and rotation fields u, v and ϕ by using cubic Hermitian functions, and the tangential deflection w and the slip deflections $2\Omega_x$, $2\Omega_s$ and $2\Omega_\kappa$ by using linear functions.

5 Applications

5.1 Comparison with experimental results

Bradford and Gilbert [27] conducted a set of experiments to determine the long-term behaviour of simply supported steel-concrete straight composite beams connected with headed shear studs. The steel section was a 200 UB 25.4 and the concrete deck had a width B_d =1000mm and a thickness t_d = 70mm which produced a total distributed vertical load of $q = 1.90$N/mm along the beam due to its self weight. An additional distributed load of $q = 7.52$N/mm was applied along the 5900mm total span and was maintained for 250 days. The stiffness of the shear studs was determined from the standard push-out test explained in [13] as $k_c = 84k$N/mm. For the first beam experiment, two shear studs were used at every 200mm along the beam (B1 beam in [27]), which corresponds to a shear stiffness of $\rho_w = 84000 \times 2/(200 \times 133) = 6.30\text{N/mm}^3$ in the composite beam model used herein in which the width of the effective interface surface between the steel girder and concrete deck is taken as 133mm. For the second beam experiment, the stud intervals were increased to 600 mm, i.e. $\rho_w = 2.10\text{N/mm}^3$ (B3 beam in [27]).

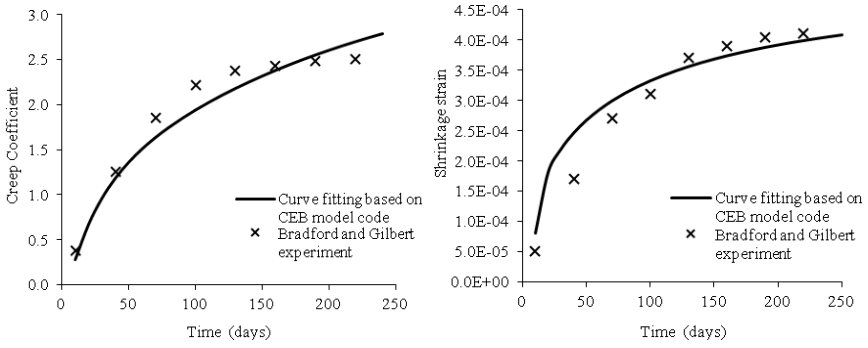

(a) Creep coefficient (b) shrinkage strain

Figure 2: Experimental and CEB curves

The steel material was assumed to be elastic with a modulus of E_s=200 kN/mm^2. The creep coefficient and shrinkage curve for the concrete material were determined by means of separate tests carried out on cylindrical specimens and determined as shown in Figure 2. The curves fitting this data were determined conveniently by using the CEB model code [28], based on which the code parameters were chosen and shown in Table 1.

Steel girder		
Section	200 UB 25.4	Section designation of the steel girder
E_s	200 kN/mm^2	Elastic modulus of the steel
G_s	77 kN/mm^2	Shear modulus of the steel
Shear studs		
ρ_w	2.10 N/mm^3	Stiffness modulus of shear connections in tangential direction
ρ_u	2.10 N/mm^3	Stiffness modulus of shear connections in radial direction
Concrete slab		
B_d	100 0mm	Width of the deck
D_d	70 mm	Depth of the deck
f_{ck}	31.1 N/mm^2	Characteristic compressive strength of the concrete
E_{c0}	25.1 kN/mm^2	Elastic modulus of the concrete on the tenth day
G_{c0}	10.0 kN/mm^2	Shear modulus of the concrete on the tenth day
ν_c	0.2	Poisson's ratio of the concrete
RH	50%	Relative humidity of the ambient environment
t_0	10 days	Age of the concrete (days) at the first loading
β_{sc}	5	Cement coefficient (β_{sc} = 5)

Table 1: Composite cross-section and material properties.

Eight elements along the span were used to model the beam in which the concrete deck was divided into 64 rectangular areas; sixteen along the width and four across the thickness as shown in Figure 3.

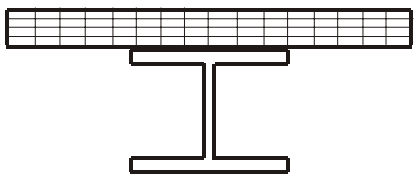

Figure 3 Sampling point scheme of the steel-concrete composite cross-section.

Evolutions of the deflections at mid-span and at the quarter point for both beams and comparisons between the experimental results and those based on the developed model are shown in Figure 4.

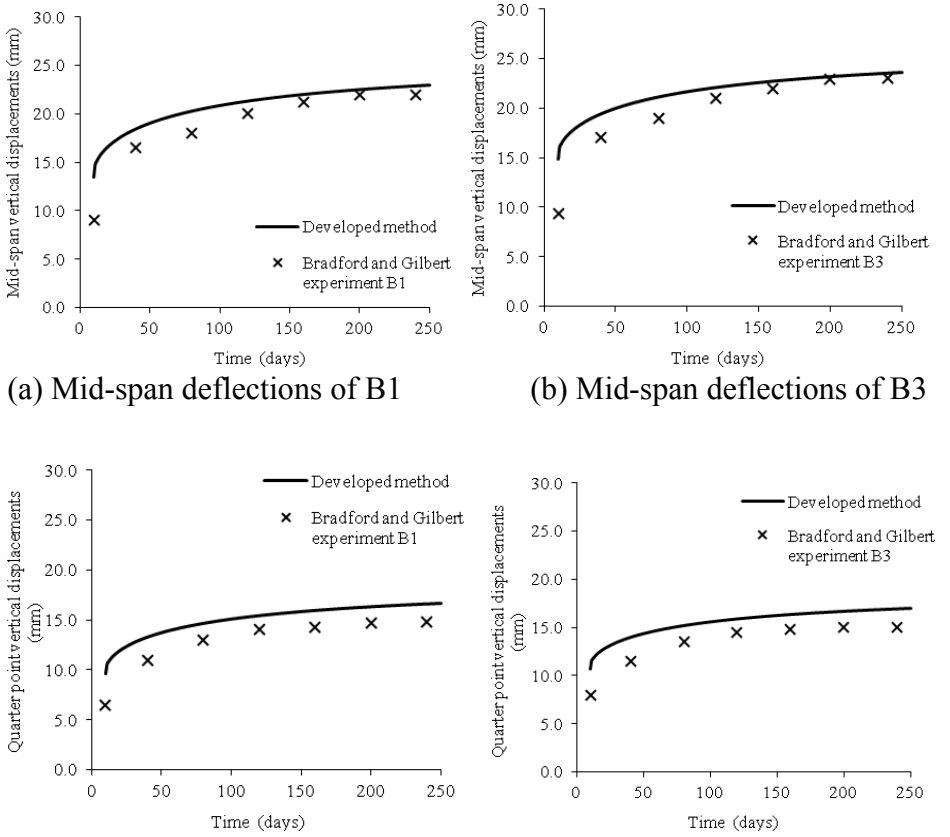

(a) Mid-span deflections of B1 (b) Mid-span deflections of B3

(c) Quarter point deflections of B1 (d) Quarter point deflections of B3

Figure 4: Time-dependent vertical deflections.

It can be seen from Figure 4 that based on the parameters chosen in Table 1 the results are in good agreement after 250 days, however a greater gap can be observed for the instantaneous response of the beams and the model depict slightly more flexible behaviour than the actual behaviour at the initiation of loading.

5.2 Comparison with ABAQUS model

In order to validate the developed method, an ABAQUS shell element model has been developed for comparison purposes, in which the creep and shrinkage effects of concrete as well as the partial interaction between the steel girder and concrete deck are taken into account. The example beam is simply supported with a total length of 5.9 m and the shear connection stiffness of $\rho_w = \rho_u = 2.10$ N/mm^3. The beam is curved in plan with an included angle of $\theta = 15°$ (Figure 1). The details of the composite cross-section and material properties are same as in the previous example (given in Table 1), with the applied distributed load being $q = 9.42$ N/mm. Similarly, eight elements were used to model the beam and the concrete deck was divided into 64 rectangular areas. On the other hand, for the ABAQUS model a total of 1300 (S4) shell elements were used as shown in Figure 5.

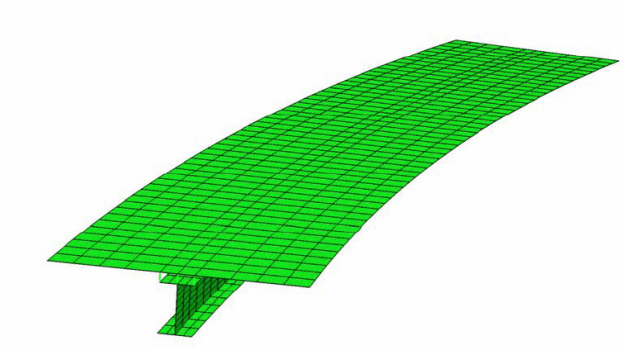

Figure 5: ABAQUS model for the curved composite beam.

Figure 6 shows the vertical and radial deflections and angles of twist at the mid-span of the beam during 250 days based on the developed model (DM) and the ABAUQS model.

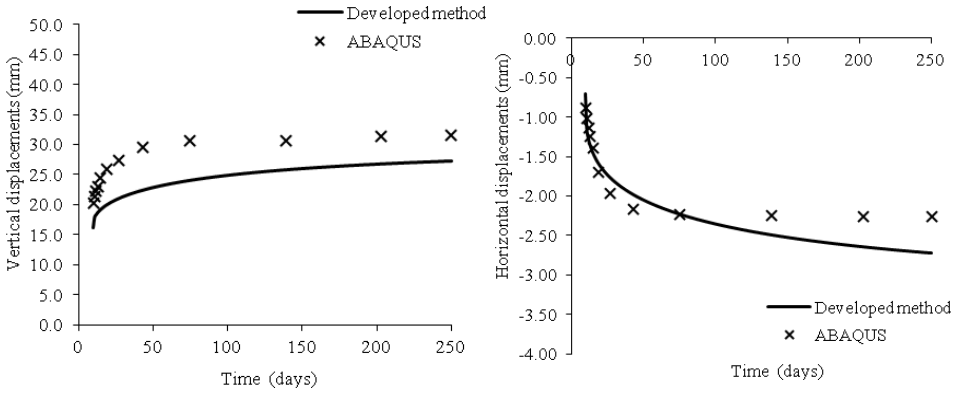

(a) Vertical deflections (b) Radial deflections

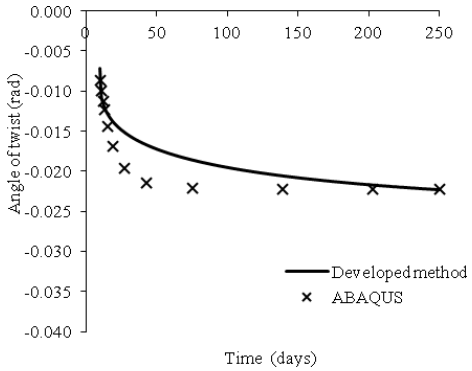

(c) Angles of twist

Figure 6: Time-dependent mid-span deflections based on the ABAQUS model and the developed method.

Spring elements were used in the tangential and radial directions to connect the concrete deck and the top flange of the steel girder in order to model the partial interaction at the deck and girder interface. Three spring elements with equal stiffness were used every 118 mm along the beam. Based on the stiffness modulus of shear connections $\rho_w = \rho_u = 2.10$ N/mm^3, the stiffness of the springs were determined as $k_c = 11$ N/mm. Truss elements with large cross-sections were used to connect the concrete deck and the top flange of the steel girder in the vertical direction in order to prevent uplifting. The vertical and radial deflections as well as the rotations were restrained at the centroid of the girder at both ends ($u = v = \phi = 0$), while the tangential displacement of the centroid is restrained only at one end ($w = 0$). Five other points of the cross-section at both ends were restrained in the vertical directions to prevent the twisting of the cross-section while allowing for warping deformations. The distributed vertical loading of $q = 9.42$ N/mm along the span was applied by using $P = 1.11$ kN nodal vertical loads at the centroid of the girder every 118 mm along the beam. The viscoelastic time analysis was performed in the ABAUQS model by defining the viscoelastic material parameters of the concrete using the VISCOELSTIC, TIME = CREEP TEST DATA command [30]. The shrinkage effect of the concrete deck was considered by using the EXPANSION command [29], in which the expansion coefficients have negative values.

5.3 Slip due to warping

As indicated in Equation (3), by using the function Ω_κ, the slip effect in the concrete slab and steel flange interface due to the warping of the cross-section is considered in this paper. In Figure 7, two cases are illustrated to show the relationship between the slip, the flange rotation angle and the function Ω_κ.

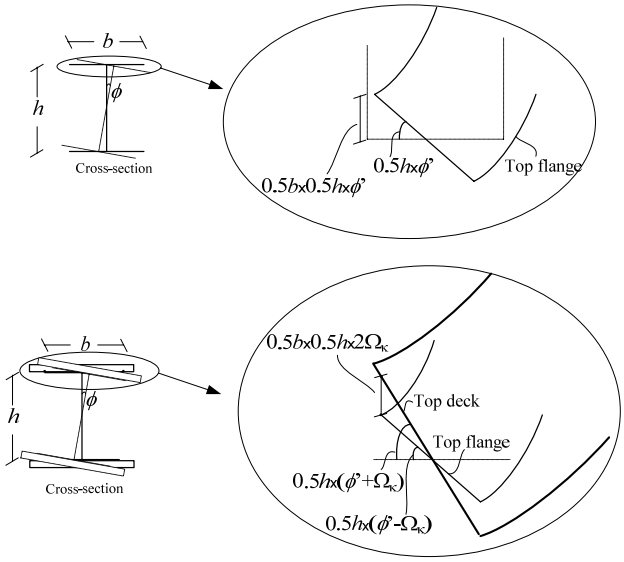

Figure 7: Warping and slip due to warping.

The cross-section for the first case is not composite and the flange rotation angle is related to the longitudinal displacement at the tip of the flange due to warping. In the second case, warping induced differences between the longitudinal displacements of the top flange and the top deck is shown for the composite cross-section which requires the function Ω_κ introduced in the beam model.

A straight composite beam model with doubly symmetric cross-section is analysed under torsional load to generate torsional behaviour only, and thus to cause slip between the components due to warping of the cross-section only. As shown in Figure 8, an ABAQUS model is also developed for comparison purposes. The beam is under uniformly distributed torsional load of m_s=100kN·mm/mm, simply-supported and has a total length of 5.9 m. The top and bottom concrete slabs of the beam are connected to the top and bottom flanges of steel girder, with flexible shear connection with a stiffness of $\rho_w=\rho_u$=0.5N/mm^3. The cross-section is forced to behave rigid in its plane during deformation in the ABAQUS model which is consistent with the kinematic assumptions of the developed beam formulation. Other details of the composite cross-section and material properties of the beam are as same as in the previous examples (given in Table 1).

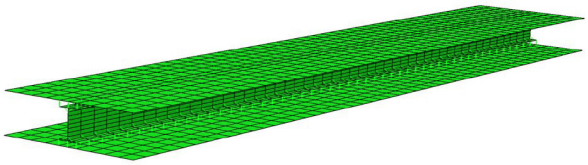

Figure 8: Straight composite beam.

Figure 9 shows the slips at the tips of the steel flanges due to warping along the length of the beam based on the ABAQUS model and the developed method (DM), from which it can be seen that the results based on the developed method are in very good agreement with the ones based on the ABAQUS model.

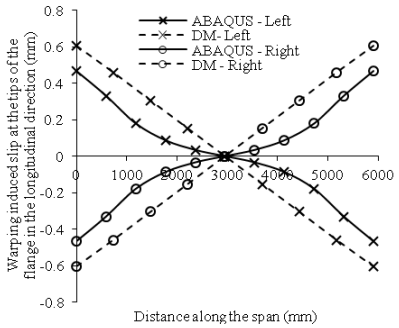

Figure 9: Warping induced slip at the tips of the flange in the longitudinal direction based on the ABAQUS model and the developed method.

On the other hand, warping induced slips at the right and left tips of the top flange are equal in value but in opposite directions, and thus average slip due to warping is zero. Thus, an independent parameter Ω_κ should be assigned to capture the slip effects due to warping.

5.4 Effects of partial interaction

In order to illustrate the effects of partial interaction on the time-dependent behaviour of composite curved beams, a group of beams with different connection stiffnesses are analysed using the developed model. Figure 10 shows the vertical and radial displacements, angle of twist, and radial and tangential slips along the beam at the initiation of the loading and after 1000 days due to external loading only and without the shrinkage effects.

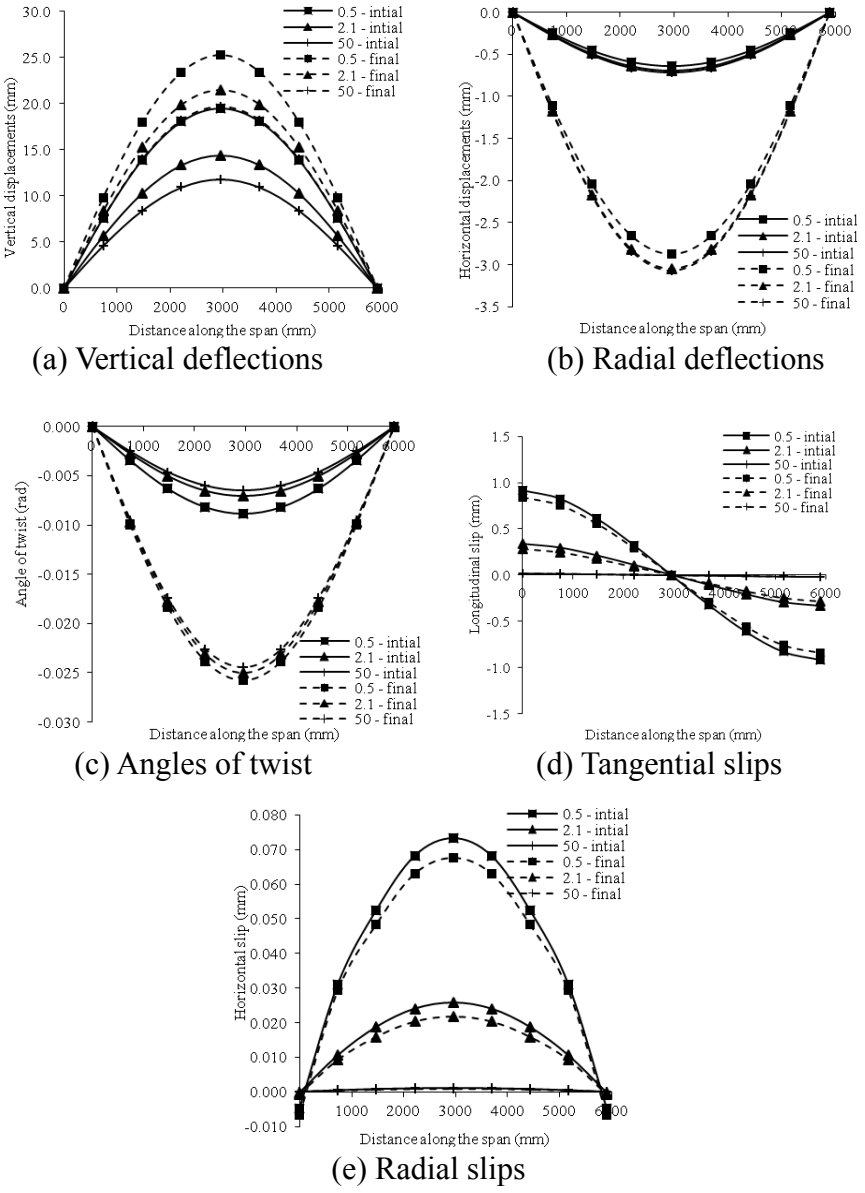

Figure 10: Deformed shapes at the initiation of loading and after1000 days for different connection stiffnesses without shrinkage effects.

The stiffness modulus of shear connections are selected as $\rho_w = \rho_u = 0.5\text{N/mm}^3$, $\rho_w = \rho_u = 2.1\text{N/mm}^3$ and $\rho_w = \rho_u = 50\ \text{N/mm}^3$ for comparison. It should be noted that $\rho_w = \rho_u = 0.5\text{N/mm}^3$ corresponds to shear connector modulus of 68 N/mm^2 which is a practical value used for shear stud connectors [3]. Figure 11 depicts the corresponding deformed shapes due to the shrinkage effect only. The results show that the directions of radial and tangential slips caused by external loads are opposite to those due to shrinkage effects.

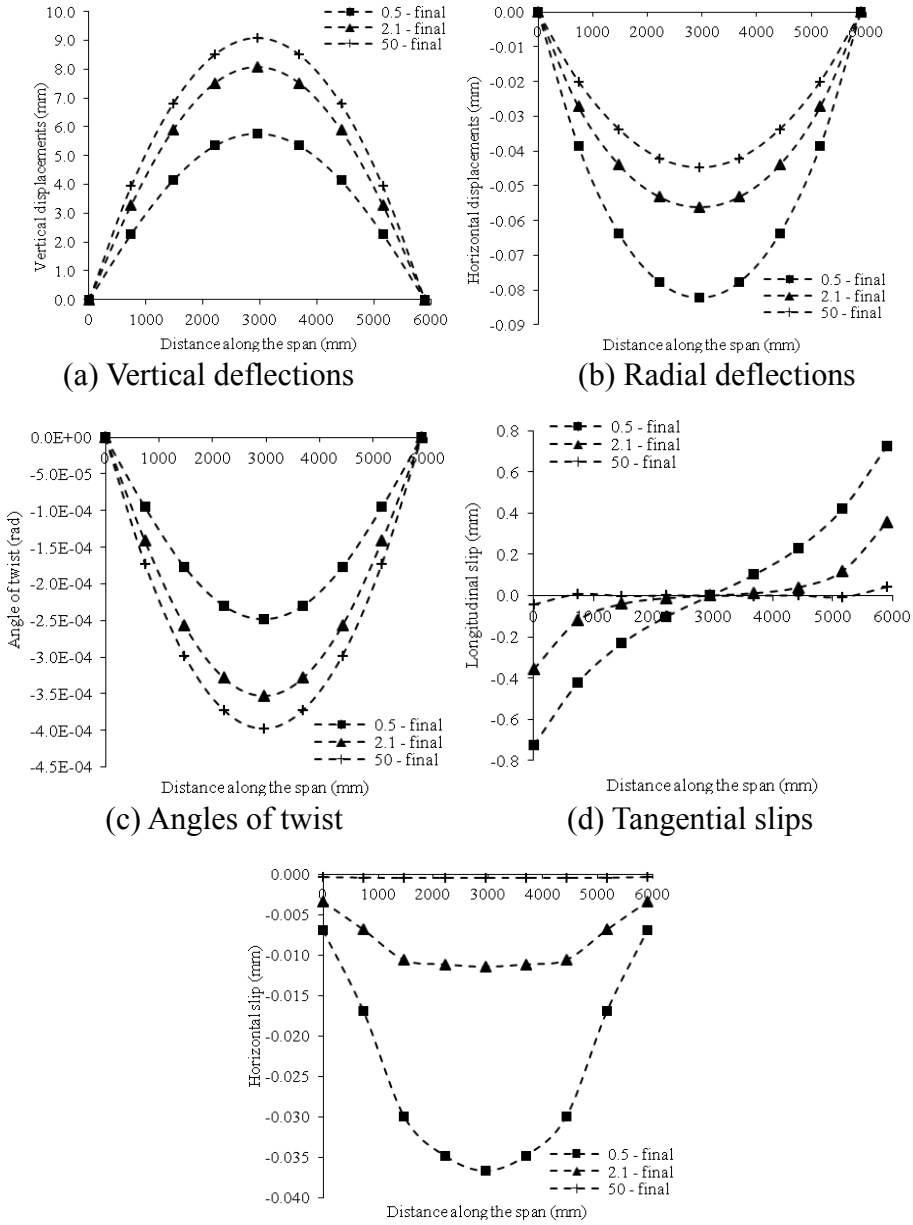

Figure 11: Deformed shapes after 1000 days for different connection stiffnesses due to shrinkage effects.

It can also be observed that, the slips in radial and tangential directions in the beam with shear connection stiffness $\rho_w = \rho_u$ =50N/mm^3 are negligible comparison to the other two beams, and that the shear connection stiffness has a clear effect on the vertical deflections and angles of twist. As shown in Figure 11, the mid-span vertical displacement at the initiation of loading, decreases 39% when the stiffness of shear connections are increased from $\rho_w = \rho_u$ =0.5N/mm^3 to $\rho_w = \rho_u$ =50N/mm^3 and after 1000 days this difference reduces to 22%. Thus, the effect of partial interaction between the composite components is more significant at the initiation of loading; however, they should be taken into account for accurate time-dependent analysis since the assumption of full interaction may underestimate the deflections.

6 Conclusions

An efficient numerical method has been developed for the creep and shrinkage analysis of steel-concrete composite beams that are curved in plan by using the age-adjusted effective modulus method. Through comparisons with available experimental results and a viscoelastic ABAQUS shell element model, it was shown that the developed formulation captures the time-dependent creep and shrinkage behaviour of composite beams. The developed method considers the effects of partial interaction between the concrete deck and the steel girder in the radial direction as well as in the tangential direction and their effect on the time-dependent behaviour of curved composite beams was investigated. It was demonstrated that the initial curvature of the beam has a significant influence on the time-dependent behaviour of composite beams. It was also shown that the effects of partial interaction between the two composite components should be taken into consideration for an accurate time-dependent analysis, since the assumption of full interaction may misestimate the deformations. In addition, the warping induced slip effect has been studied. In this study, it is clearly shown that an independent parameter is required to capture the warping induced tangential slip as considered by the beam model adopted herein.

Acknowledgements

The work in this paper was supported by the Australian Research Council through a Discovery Project award to the third author. The support is gratefully acknowledged.

References

[1] F. Giussani, F. Mola, “Service-stage analysis of curved composite steel-concrete bridge beam”, Journal of Structural Engineering, ASCE, 132(12), 1928-1939, 2006.

[2] D.J. Oehlers, M.A. Bradford, “Composite steel and concrete structural members: Fundamental behaviour’, Pergamon, Oxford, 1995.

[3] D.J. Oehlers, M.A. Bradford, “Elementary behaviour of composite steel and concrete structural members”, Butterworth-Heinemann, Oxford, 1999.

[4] N.M. Newmark, C.P. Siess, I.M. Viest, “Tests and analysis of composite beams with incomplete interaction”, Proceedings of the Society for Experimental Stress Analysis, 9(1), 75-92, 1951.

[5] R.E. Erkmen, M.A. Bradford, “Nonlinear elastic analysis of composite beams curved in-plan”, Engineering Structures, 31, 1613-1624, 2009.

[6] Standards Australia (SA), “Australian Standard AS2327.1 Composite structures – Part 1: Simply supported beams”, Sydney, Australia, 2003.

[7] M.A. Bradford, B. Uy, Y.L. Pi, “Behaviour of unpropped composite girders curved in plan under construction loading”, Engineering Structures, 23, 779-789, 2001.

[8] A.M. Tarantino, L. Dezi, “Creep effects in composite beams with flexible shear connectors”, Journal of Structural Engineering, ASCE, 118(8), 2063-2081, 1992.

[9] L. Dezi, A.M. Tarantino, “Creep in composite continuous beams I: Theoretical treatment”, Journal of Structural Engineering, ASCE, 119(7), 2095-2111, 1993.

[10] L. Dezi, A.M. Tarantino, “Creep in composite continuous beams II: Parametric study”, Journal of Structural Engineering, ASCE, 119(7), 2112-2133, 1993.

[11] L. Dezi, F. Gara, G. Leoni, A.M. Tarantino, “Time-dependent analysis of shear-lag effect in composite beams”, Journal of Engineering Mechanics, 127(1), 71-79, 2001.

[12] Z.P. Bazant, “Numerical determination of long-range stress history from strain history in concrete”, Materials and Structures, 5(27), 135-141, 1972.

[13] M.A. Bradford, R.I. Gilbert, “Composite beams with partial interaction under sustained loads”, Journal of Structural Engineering, ASCE, 118(7), 1871-1883, 1992.

[14] R.I. Gilbert, M.A. Bradford, “Time-dependent behaviour of continuous composite beams at service loads”, Journal of Structural Engineering, ASCE, 121(2), 319-327, 1995.

[15] L. Dezi, G. Leoni, A.M. Tarantino, “Algebraic method for creep analysis of continuous composite beams”, Journal of Structural Engineering, ASCE, 122(4), 423-430, 1996.

[16] G. Ranzi, M.A. Bradford, “Analysis solutions for the time-dependent behaviour of composite beams with partial interaction”, International Journal of Solids and Structures, 43, 3770-3793, 2005.

[17] C. Amadio, M. Fragiacomo, “Simplified approach to evaluate creep and shrinkage effects in steel-concrete composite beams”, Journal of Structural Engineering, ASCE, 123(9), 1153-1162, 1997.

[18] R.E. Erkmen, M.A. Bradford, “Time-dependent creep and shrinkage analysis of composite beams curved in-plan”, Computers & Structures, 89, 67-77, 2011.

[19] R.E. Erkmen, M.A. Bradford, “Non-linear quasi-viscoelastic behaviour of composite beams curved in-plan”, Journal of Engineering Mechanics, ASCE, 137, 238-247, 2011.

[20] R.T. Gilbert, “Time Effects in Concrete Structures”, Elsevier, Amsterdam, 1988.
[21] Z.P. Bazant, B.H. Oh, “Deformation of progressively cracking reinforced concrete beams”, Journal of ACI, 81, 268-278, 1984.
[22] D. McHenry, “A new aspect of creep in concrete and its application to design”, Proceedings of ASTM, 43, 1069-1086, 1943.
[23] SA (Standards Australia), “Australian Standard AS 3600 Concrete Structures”, Sydney, Australia, 2001.
[24] Z.P. Bazant, “Prediction of concrete creep effects using age-adjusted effective modulus method”, Journal of ACI, 69, 212-217, 1972.
[25] CEB (Comité Euro-International du Béton), “CEB Design manual on structural effects of time dependent behaviour of concrete”, Georgi Publishing, Saint-Saphorin, Switzerland, 1984.
[26] M. Jirasek, Z.P. Bazant, “Inelastic analysis of structures”, John Wiley & Sons, New York, 2002.
[27] M.A. Bradford, R.I. Gilbert, “Time-dependent behaviour of simply-supported steel concrete composite beams”, Magazine of Concrete Research, 43(157), 265-274, 1991.
[28] CEB-FIB (Comité Euro-International du Béton – Fédération International de la Précontrainte), “Mode Code 1990: Design Code”, Thomas Telford, London, UK, 1993.
[29] H.D. Hibbit, B.I. Karlsson, E.P. Sorensen, “ABAQUS User’s manual Version 6.8”, Hibbitt, Karlsson & Sorensen Inc., Pawtucket, USA, 2008.